ETC HE Report 2022/23

Evaluation of European-wide map creation of flux-based ozone indicator POD for selected tree species

Authors:
Leona Vlasáková (CHMI), Jana Marková (CHMI), Frédéric Tognet (INERIS), Jan Horálek (CHMI), Augustin Colette (INERIS)

European Environment Agency
European Topic Centre
Human health and the environment

Cover design: EEA
Cover image © Leona Vlasáková
Layout: CHMI

Publication Date: March 2023
Revised Version - Publication Date: 21 February 2024
ISBN 978-82-93970-40-8

How to cite this report:
Vlasáková, L., Marková, J., Tognet, F., Horálek, J., Colette, A. (2022). *Evaluation of European-wide map creation of flux-based ozone indicator POD for selected tree species* (Eionet Report – ETC HE 2022/23). European Topic Centre on Human Health and the Environment.

Revision note
This is a revised version of the report published in March 2023, which has been prepared due to an error in the ozone measurement data. Map 4.1 and its description have been updated.

ETC HE coordinator: Stiftelsen NILU
(https://www.nilu.com/)

ETC HE consortium partners: Federal Environment Agency/Umweltbundesamt (UBA), Aether Limited, Czech Hydrometeorological Institute (CHMI), Institut National de l'Environnement Industriel et des Risques (INERIS), Swiss Tropical and Public Health Institute (Swiss TPH), Universitat Autònoma de Barcelona (UAB), Vlaamse Instelling voor Technologisch Onderzoek (VITO), 4sfera Innova S.L.U., klarFAKTe.U

European Topic Centre on
Human health and the environment (ETC HE)
https://www.eionet.europa.eu/etcs/etc-he

Contents

Acknowledgements

The ETC HE task manager was Jan Horálek (CHMI). The EEA project manager was Alberto González Ortiz. Other contributors were Leona Vlasáková, Jana Marková (both CHMI), Frédéric Tognet and Augustin Colette (both INERIS). Additional input was provided by Daša Damašková, Pavel Kurfürst (both CHMI) and Florian Couvidat (INERIS). Thanks are due to Patrick Büker (GIZ) from ICP Vegetation (UNECE Convention on Long-Range Transboundary Air Pollution) for valuable reviewing and comments on the report.

For the POD calculations, the module to estimate phytotoxic ozone doses from a given atmospheric ozone exposure developed by INERIS has been used (Colette et al., 2018).

This work has been partly funded by the Czech national project ARAMIS – Integrated system of research, evaluation and control of air quality (co-funded with the state support of the Technology Agency of the CR under the Environment for Life program).

Summary

It is widely acknowledged that the impacts of ground-level ozone (O_3) on vegetation – including trees – are more closely related to the instantaneous O_3 flux or O_3 dose absorbed through the stomata than to exposure to specific concentrations of O_3 in the atmosphere since only the O_3 molecules that enter the leaves through the stomata are harmful to plants.

Therefore, an index based on stomatal O_3 uptake (i.e. POD_Y) that accumulates O_3 flux entering into the leaves via stomata is more appropriate than the O_3 concentration-based metric. Flux-based critical levels (CLs) derived for the phytotoxic O_3 dose (POD) were introduced by the Convention on Long-Range Transboundary Air Pollution (CLRTAP); the last revision took place in 2017 (CLRTAP, 2017a).

This paper examines the potential inclusion of Phytotoxic Ozone Dose (POD) for selected tree species in regular mapping under the ETC HE. The paper concludes that the inclusion of POD for trees in the routine mapping together with other regular maps is feasible, i.e. such maps show reasonable results and their creation is technically possible.

The POD maps for the 2020 growing season for selected trees, i.e. beech (*Fagus sylvatica*) and spruce (*Picea abies*), are created with calculated hourly POD values which are based on hourly O_3 concentrations, hourly meteorological parameters such as temperature, vapour pressure deficit, solar radiation and soil hydraulic property data. The hourly O_3 concentrations are calculated by combining the monitoring data from rural background stations, chemical transport modelling data and other supplementary data (Horálek et al., 2022).

POD_1 (where 1 represents the hourly detoxification threshold) is calculated using the methodology described in the Manual for modelling and mapping critical loads & levels of the CLRTAP in its 2017 revision (CLRTAP, 2017a). A module to estimate phytotoxic O_3 doses from a given atmospheric O_3 exposure as developed for the Continental biogeographical region (Map A2.1) by the French National Institute for Industrial Environment and Risks (INERIS) has been used (Colette et al., 2018). This script (written in the R programming language) has been consolidated and finalized by the Czech Hydrometeorological Institute (CHMI) for use in the European-wide POD spatial calculation for selected trees, i.e. it has been modified also for the Boreal region in the case of spruce and for the Mediterranean region in the case of beech.

CLs for POD_1 for beech and spruce have been exceeded in the 2020 growing season almost throughout the whole European area considered (i.e. mapped), with the exception of large areas in northern Europe in the case of spruce, some areas in the Iberian Peninsula, Romania and Turkey in the case of beech, and other smaller areas in different countries in the case of both the beech and spruce.

1 Introduction

Ground-level ozone (O_3) is a secondary pollutant formed in a complex photochemical chain reaction from its precursors, such as nitrogen oxides (NO_X), volatile organic compounds (VOC), carbon monoxide (CO) and methane (CH4). These precursors come from both natural and anthropogenic sources. As ground-level O_3 is a photochemical pollutant, it is dependent on solar radiation intensity. Photochemical reactions of ozone precursors under high temperatures lead to ozone formation (e.g. Seinfeld and Pandis, 2006; Coates et al., 2016). Regarding precursors, not only the absolute amount of precursors but also their relative ratio is important for the formation of ground-level ozone (Sillman et al., 1990).

Future scenarios of ozone concentrations in Europe predict both increases and decreases, depending of course on the scenario inputs (Cape, 2008; Varostos et al., 2013; Hendriks et al., 2016). It is a complex issue and quantification of future levels of ground-level ozone remains uncertain due to the interaction of the many processes influencing ozone formation. There are two main drivers for future ozone concentrations; changes in meteorological conditions due to climate change potentially resulting in an increase in ozone concentration and the achievement of a sufficient reduction of the ozone precursors potentially resulting in a decrease in ozone concentration (EEA, 2015; Hendriks et al., 2016). However, it should be noted that the reduction of ozone concentrations will require a great effort in terms of reducing the precursors in order to reduce the impact of ozone on vegetation, ecosystems and human health in the future (The Royal Society, 2008). According to Hendriks et al. (2016) "if strong global action to reduce air pollutant emissions is taken, ozone damage in 2050 could be lower than at present".

O_3 is considered to be the most damaging common air pollutant for vegetation with adverse effects on crop yields and forest health (e.g. Ashmore, 2005; Paoletti and Manning, 2007; Cieslik, 2009; Mills et al., 2011; Fares et al., 2018). O_3 penetrating the stomata causes an oxidative effect resulting in plant damage. Damages to plants occur when the molecule penetrates stomata and rapidly reacts in the intercellular spaces (Fares et al., 2018). After O_3 enters through the stomata, it diffuses in the apoplast and rapidly decomposes to the hydroxyl radical $HO^{\cdot}$, superoxide anion radical O_2^{-}, hydrogen peroxide H_2O_2 and other reactive oxygen species (ROS) (Pell et al., 1997; Schraudner et al., 1997, Mittler, 2002). If the antioxidative system and the protection against the O_3-induced oxidative system are not sufficient, biochemical and physiological changes in plants occurred (Fares et al., 2013) and the plant is damaged (Ashmore, 2003). The O_3 uptake is coupled with a reduction of the Rubisco amount (Vollenweider et al., 2003; Wittig et al., 2009) resulting in cell death or premature leaf senescence and leaf loss (Pell et al., 1997; Gill and Tuteja, 2010; Long and Naidu, 2002).

O_3 may induce injury at cell, organism or ecosystem levels (Stanners and Bourdeau eds., 1995). There are a large number of studies regarding the adverse effects of O_3 on biochemical and physiological changes in plants. Typical adverse effects are visible leaf injury, accelerating leaf senescence, declining leaf chlorophyll content, reduced photosynthetic activity, reduction in carbon assimilation, biomass reduction, crown defoliation, carbon sequestration (e.g. Pell et al., 1997; Ashmore, 2003; Schaub et al., 2005; Wittig et al., 2009; Fares et al. 2013; Hoshika et al., 2013; Sicard et al., 2016; DeMarco et al., 2017; Paoletti et al., 2019). Consequently, plants weakened by the negative effects of O_3 are more sensitive to other abiotic and biotic stressors (Jones et al., 2004; De Marco et al., 2017; Dalstein et al., 2019).

All O_3 adverse effects may lead to long-term effects on ecosystem structure and function. Additionally, O_3 may also contribute to climate change in the coming years by the mechanism of plant damage due to O_3, reducing the land carbon sink for CO_2 and therefore increasing the rate at which CO_2 increases in the atmosphere (e.g. The Royal Society, 2008; Oliver et al., 2018; Zhang et al., 2022). Consequently, there is an urgent need to better understand interactions between air pollution, including O_3, and climate change-related events (Michel et al., 2021). Last but not least, it is important to consider the economic loss since the O_3 uptake is a threat for the timber production (Karlsson et al., 2005; Feng et al., 2019; Sacchelli et al., 2021).

Clearly, to protect forests against O_3 pollution appropriate standards are needed. Currently, the indicator used in the European Directive 2008/50/EC to protect vegetation against negative impacts of O_3 is the Accumulated Dose of O_3 Over a Threshold of 40 ppb (AOT40)([1]).

Critical levels for O_3 defined as AOT40 were agreed at a workshop in Kuopio, Finland in 1996 (Kärenlampi and Skärby, 1996). The approach is based on measured ambient O_3 concentrations > 40 ppb (i.e. 80 µg/m^3 under standard atmospheric conditions), regardless of whether O_3 is actually absorbed by the vegetation causing subsequent damage. The use of the AOT40 exposure index was introduced largely for practical reasons (Fuhrer, 1997; Gerosa et al., 2003). However, AOT40 does not provide any information on the physiological O_3 uptake into the leaves since it does not take into account any environmental factors affecting the O_3 uptake via stomata (Anav et al., 2016). The stomatal O_3 flux approach, in contrast to the concentration based approach, provides an estimate of the critical dose of O_3 entering via stomata and takes into account the main environmental conditions influencing stomatal O_3 uptake, such as phenology, air temperature, soil moisture, vapour pressure deficit (VPD) and solar radiation (Emberson et al., 2000). In other words, high ambient O_3 concentrations may not injure plants when stomata are closed (Ronan et al., 2020) during unfavourable conditions i.e. high vapour pressure deficit, high temperature and low soil humidity (Agyei, 2020; Paoletti, 2006). Conversely, relatively low O_3 concentrations can still lead to fairly high O3 fluxes when stomata are open under favourable environmental conditions (Matyssek et al., 2007), thereby resulting in damage of the vegetation (Karlsson et al., 2017).

The study of Proietti et al. (2021) showed a significant decrease of O_3 concentrations and an exposure-based index, namely AOT40, due to successful control strategies to reduce the emission of O_3 precursors in Europe since the early 1990s. In contrast, the stomatal O_3 uptake by forests increased, leading to an increase of potential O_3 damage to plants in Europe. A similar conclusion was reported by Ronan et al. (2020) who found a decrease in concentration-based metrics over 2005-2014 at most sites in the USA and Europe but an increase in phytotoxic ozone dose (POD) in forests. Reasons for POD increases despite the reduction in O_3 concentrations are that stomatal conductance is influenced by environmental variables (Ronan et al., 2020) and climate change i.e. a longer growing season and the positive effect of air temperature on stomatal opening (Anav et al., 2019; Proietti et al.,2021).

For all these reasons, it is widely acknowledged that the impacts of O_3 are more closely related to the instantaneous O_3 flux or O_3 dose absorbed through the stomata than to O_3 exposure in the ambient air, since only O_3 molecules that enter the leaves through the stomata are harmful to plants (e.g. Musselman and Massman, 1998; Nussbaum et al., 2003; Fares et al., 2010; Musselman et al., 2006; Matyssek et al., 2007, Cieslik, 2009). Fares et al. (2010) suggested that AOT40 is a poor predictor of stomatal O_3 uptake, and that a physiologically based metric would be more effective. Therefore, an index based on stomatal O_3 uptake such as POD_Y, which considers the accumulated O_3 flux entering into the leaves via stomata above a threshold Y, is more appropriate than a purely O_3 concentration-based metric. Subsequently this flux-based POD_Y (i.e. the accumulated stomatal O_3 flux above detoxification threshold Y) measure was adapted by the Convention on Long-Range Transboundary Air Pollution (CLRTAP, 2017a; Mills et al., 2011).

The cumulative stomatal ozone fluxes (F_{sto}) through the stomata of leaves found at the top of the canopy are calculated over the course of the growing season based on ambient ozone concentration and stomatal conductance (g_{sto}) to ozone. The stomatal conductance has been calculated using a multiplicative stomatal conductance model (Emberson et al., 2000) based on Jarvis (1976) as a function of species-specific maximum g_{sto} (expressed on a single leaf-area basis), phenology, and prevailing environmental conditions - photosynthetic photon flux density, PPFD, air temperature, vapour pressure deficit (VPD), and soil moisture. Phenology and soil moisture are supposed to be the key factors for the stomatal conductance (CLRTAP, 2017a). Phenology is a primary driver of the seasonality of fluxes. The most important phenological periods to define for forests trees are the start and end of the physiologically active growth

([1]) AOT40 means the sum of the differences between hourly concentrations greater than 80 µg/m^3 (= 40 parts per billion) and 80 µg/m^3.

period (Tuovinen, 2009). The importance of taking into account soil moisture conditions for the O_3 flux calculations using the method published by CLRTAP was highlighted by Büker et al. (2012). Consequently it is possible to calculate the Phytotoxic O_3 Dose above a threshold flux Y (POD_Y). Y represents the hourly detoxification threshold below which every molecule of O_3 that enters through the stomata is expected to be degraded without causing any damage (Musselman et al., 2006; Jakovljević, 2021).

A uniform O_3 flux threshold of Y = 1 nmol/m^2/s PLA (projected leaf area) was adopted for use in species-specific phytotoxic O_3 doses above a threshold of Y (POD_YSPEC) for all tree species at the O_3 Critical Levels workshop in Madrid, November 2016 (CLRTAP, 2017a), based on data and analyses presented in Büker et al. (2015). POD_YSPEC is a POD_Y specific to a species or group of species requiring comprehensive input data, thus making it suitable for detailed risk assessment. For applications in a climate change context, the POD_YSPEC method is recommended as key factors such as phenology, regulating the gas exchange between biosphere and atmosphere (Anav et al., 2017), and soil moisture are included in the parameterisation (CLRTAP, 2017a). Anav et al. (2022) illustrated that POD_1 is the most reliable simple estimate of O_3 risk and recommended the use of this metric by policy makers as an air quality standard to protect vulnerable forest ecosystems in the future.

The monitoring of O_3 flux and the estimation of exceedances of critical levels for terrestrial ecosystems in order to assess O_3 damage to vegetation growth and biodiversity is recommended by Annex V of the Directive (EU) 2016/2284 on the reduction of national emissions of certain atmospheric pollutants (EU, 2016) and by the Commission Notice on ecosystem monitoring under Article 9 and Annex V of Directive (EU) 2016/2284 of the European Parliament and of the Council on the reduction of national emissions of certain atmospheric pollutants (NEC-Directive) (EU, 2019). According to Anav et al. (2016), in light of inconsistencies between AOT40 and POD_y, using AOT40 because of its relative simplicity is no longer justified. Further studies concerning the effect of O_3 on plants and the subsequent damage leading to economic losses should not rely on concentration-based approaches, but take into account conclusions drawn from flux-based approaches (Ronan et al., 2020). Moreover, a biologically-sound stomatal flux-based standard (POD_Y) as a new European legislative standard is needed in a climate change context (Proietti et al., 2021).

Following the inclusion of the Phytotoxic Ozone Doze (POD) for crops in regular mapping (Horálek et al., 2021), the feasibility of potential regular mapping of the POD for selected trees is evaluated in this report. POD is calculated using the methodology described in the Manual for modelling and mapping critical loads & levels of the CLRTAP in its 2017 revision (CLRTAP, 2017a). The feasibility of a routine calculation of POD for trees together with other regular maps is examined. The POD for selected European trees species, namely beech (*Fagus sylvatica*) and spruce (*Picea abies*), is calculated for the whole of Europe for the 2020 vegetation period.

As in the case of the creation of POD maps for crops (Horálek et al., 2022), the hourly ozone gridded data calculated by combining the monitoring, chemical transport modelling, and other supplementary data have been used in the POD for trees mapping. The methodology for the spatial ozone data calculation is a linear regression model followed by kriging of the residuals from that regression model (residual kriging), which is primarily driven by the monitoring data. Only ozone monitoring data from rural background stations are used, similarly to the mapping of other vegetation-related indicators (Horálek et al., 2022). Thus, the maps are labelled as rural, being representative for rural areas only.

Chapter 2 describes the methodology and routines used in the calculations. Chapter 3 documents the input data applied to the POD mapping. Chapter 4 presents and discusses the results – maps of POD for beech and spruce trees. Chapter 5 presents the conclusions. Annexes 1 and 2 document the technical details of the POD calculations.

2 Methods and routines used

2.1 Phytotoxic Ozone Dose above a threshold flux Y (PODy) for trees

The calculation of the phytotoxic O_3 dose above a threshold Y (POD_Y) as described below follows precisely the methodology described in the Manual for modelling and mapping critical loads & levels of the CLRTAP in its most recent available revision (CLRTAP, 2017a), including some specifications presented in the Scientific background documents of this manual (CLRTAP, 2017b, 2020), as prepared by the International scientific Cooperative Programme on effects of air pollution on natural vegetation and crops of the Working Group on Effects of the CLRTAP (ICP Vegetation).

The steps to be taken are presented in Table 2.1. This paper deals with step 1-5.

Table 2.1: Steps to be taken to calculate exceedance of flux-based (POD_YSPEC or POD_YIAM) critical levels

1	Decide on the species and biogeographical region(s) to be included.
2	Obtain the O_3 concentrations at the top of the canopy for the species or vegetation-specific accumulation period.
3	Calculate the hourly stomatal conductance of O_3 (g_{sto}).
4	Model the hourly stomatal flux of O_3 (F_{sto}).
5	Calculation of POD_Y (POD_YSPEC or POD_YIAM) from F_{sto}.
6	Calculation of exceedance of flux-based critical levels.

* POD_YSPEC is a species or group of species-specific POD_Y that requires comprehensive input data and is suitable for detailed risk assessment. POD_YIAM is a vegetation-type specific POD_Y that requires less input data and is suitable for large-scale modelling, including integrated assessment modelling.

Source: CLRTAP, 2017a.

The cumulative stomatal O_3 fluxes (F_{sto}) are calculated over the course of the growing season by multiplying the ambient O_3 concentration with the corresponding stomatal conductance (g_{sto}) to O_3. g_{sto} is calculated using a multiplicative stomatal conductance model proposed by Jarvis (1976) and modified by Emberson et al. (2000) as a function of species-specific maximum g_{max} (expressed on a single leaf-area basis), phenology, and prevailing environmental conditions - photosynthetic photon flux density (PPFD), air temperature, vapour pressure deficit (VPD), and soil moisture.

Hourly averaged stomatal O_3 fluxes (F_{sto}) in excess of a threshold Y, expressed in mmol/m^2 PLA ([2]), are summed over a species-specific or vegetation-specific accumulation period, in order to get the phytotoxic O_3 dose above the threshold *Y* (POD_Y) using the equation:

$$POD_Y = \sum_n (F_{sto}(n) - Y) \cdot \frac{3600}{10^6} \qquad \text{(mmol/m}^2\text{ PLA)} \qquad \text{(Eq. 1)}$$

where the threshold value Y (nmol/m^2 PLA per second) is subtracted from each hourly averaged F_{sto} (nmol/m^2 PLA per second) value only when $F_{sto} > Y$, and only during daylight hours which are assessed as when global radiation is more than 50 W/m^2.

Two POD_1 versions are available: POD_1IAM is a vegetation type specific version of POD for Integrated Assessment Modelling. We preferred to use here POD_1SPEC, which is specific to a given species – beech (*F. sylvatica*) and Norway spruce (*P. abies*) being the species in this case.

([2]) PLA, or the projected leaf area, is the total area of the sides of the leaves that are projected towards the sun. PLA is different to the total leaf area, which accounts for both sides of the leaves.

As can be seen in Eq. 1, the accumulated stomatal O_3 fluxes in excess of the threshold Y is converted to hourly fluxes by multiplying by 3 600 and to mmol by dividing by 10^6, to get the stomatal O_3 flux in mmol/m^2 PLA. A uniform O_3 flux threshold of Y = 1 nmol/m^2 PLA per second was adopted for all tree species using POD_1SPEC for the calculation of POD.

2.1.1 Decision on the species and biogeographical region(s) to be included

Plant stomatal functioning varies per plant species and can vary by biogeographical region, reflecting different adaptations of plants to climate and soil water in these regions. To accommodate these differences, separate parameterisations and accumulation periods have been developed for stomatal O_3 flux models for different species and biogeographical regions. The EEA classification([3]) of biogeographical zones is recommended for application to risk assessments for Europe (for details see Annex 2). Parametrization for POD_1 for beech and Norway spruce is currently available for different biogeographic regions of Europe apart from Alpine region, i.e. for Atlantic, Boreal (only for Norway spruce), Continental, Pannonian, Steppic, and Mediterranean (only for beech) regions (CLRTAP, 2017a; CLRTAP, 2020). The parametrization is the same for most of these regions (namely Continental, Atlantic, Steppic, Pannonian), while for Boreal (in the case of spruce) and Mediterranean (in the case of beech) regions it is different. Thus, these areas are calculated separately.

Since no parametrization for beech in the Boreal, Arctic (Iceland in the mapped European area) and Alpine > 50° biogeographical regions is available, these areas are marked in lighter colours. Nevertheless, for the purpose of completeness, the POD_1 has been modelled for these regions using the parameterization for the Continental biogeographical regions. For other regions with no available parametrisation i.e. the Alpine < 50°, Anatolian and Black Sea regions, we used the parametrisations for Continental and Mediterranean regions, respectively. A more detailed overview of the parameterization used for different regions can be found in Annex 1 and Annex 2.

Since no parametrization for spruce in the Mediterranean, Anatolian and Black Sea biogeographical regions is available, these areas are also marked in lighter colours. However, again for the purpose of completeness, the POD_1 has been modelled for the Mediterranean region using the parameterization for the Continental biogeographical regions. For other regions with no available parametrisation, i.e. the Arctic and Alpine > 50°, and Alpine < 50° regions, we used parametrisations for the Boreal and Continental regions, respectively. A more detailed overview of the parameterization used for different regions can be found in Annex 2.

This report is limited to beech and Norway spruce, although the methodology presented is also applicable to other crops and vegetation (CLRTAP, 2017a). Beech and Norway spruce were selected as the tree species for which the most comprehensive parameterization for POD is available.

2.1.2 Obtaining the O_3 concentrations at the top of the canopy for the species or vegetation-specific accumulation period

For forests, O_3 concentrations must often be derived from measurements made over grasslands or other types of land cover. Conversion of O_3 concentrations at measurement height to canopy height can be best achieved with an appropriate deposition model (CLRTAP, 2017a; CLRTAP, 2017b). However, as obtaining the O_3 concentration at the top of trees in comparison to crops is rather complex and data demanding, we decided to use a simpler tabulation of O_3 gradients instead. This tabulation of O_3 gradients is also recommended and allowed by CLRTAP (2017a) and is calculated by

([3]) See http://www.eea.europa.eu/data-and-maps/data/biogeographical-regions-europe-3.

$$c(z_{tgt}) = c(z_{m,O3}) * [g(z_1) / g(z_{m,O3})] = c(z_{m,O3}) * [1 / 0.95] \quad \text{(Eq. 2)}$$

where $c(z_{tgt})$ is the concentration of O_3 at canopy top (ppb),
$c(z_{m,O3})$ is the O_3 concentration measured at the height z_m (ppb),
$g(z_1)$ is the O_3 concentration gradient for the height of canopy, i.e. 1 for trees of 20 m height,
$g(z_{m,O3})$ is the O_3 concentration gradient for the height of O_3 measurement, i.e. 0.95 for O_3 concentration measuring at height of 2 m (i.e the height of O_3 measuring equipment), assessed over grasslands for rural stations.

2.1.3 Calculation of the hourly stomatal conductance of O_3 (g_{sto})

The basis of the approach used for calculating phytotoxic O_3 doses is the calculation of an instantaneous stomatal conductance g_{sto} in the given hour H, according to the equation

$$g_{sto} = g_{max} * [\min(f_{phen}, f_{O3})] * f_{light} * \max[f_{min}, (f_{temp} * f_{VPD} * f_{SW})] \quad \text{(Eq. 3)}$$

where g_{sto} is the actual stomatal conductance (mmol O_3/m^2 PLA per second),
g_{max} is the species-specific maximum stomatal conductance (mmol O_3/m^2 PLA per second); see Annex 1),
f_{phen} is the relative proportion function for the phenology for the different growth stage,
f_{O3} is the relative proportion function for the influence of O_3 on stomatal flux by promoting premature senescence, not included for trees; a function is included only for crops,
f_{min} is the relative minimum stomatal conductance that occurs during daylight hours,
f_{temp}, f_{VPD}, f_{SW}, f_{light} are relative proportion functions for leaf stomata response to temperature, air humidity, soil moisture and light.

Parameters f_{phen}, f_{light}, f_{temp}, f_{VPD}, f_{SW} and f_{min} are expressed as relative proportion functions, taking values between 0 and 1 as a proportion of g_{max}. These functions allow taking into account irradiance (f_{light}), temperature (f_{temp}), water vapour deficit at leaves level (f_{vpd}), soil moisture (f_{sw}), the phenology for the different growth stage (f_{phen}) and the influence of O_3 on stomatal flux by promoting premature senescence (f_{O3}).

For forest trees, f_{phen} is calculated using parameterisations based on a fixed number of days. Each pair of equations gives f_{phen} in relation to the yearly accumulation period for POD_YSPEC where A_{start} and A_{end} are respectively the start and end of the accumulation period which here is the growing season.

The parameter f_{phen} is calculated according to:

$$f_{phen} = (1 - f_{phen\_a}) * [(yd - A_{start})/f_{phen\_1\_FD}] + f_{phen\_a} \quad \text{for} \quad A_{start\_FD} \le yd < (A_{start} + f_{phen\_1\_FD}) \quad \text{(Eq. 4)}$$

$$f_{phen} = 1 \quad \text{for} \quad (A_{start} + f_{phen\_1\_FD}) \le yd \le (A_{end} - f_{phen\_4\_FD}) \quad \text{(Eq. 5)}$$

$$f_{phen} = (1 - f_{phen\_e}) * [(A_{end} - yd)/f_{phen\_4\_FD}] + f_{phen\_e} \quad \text{for} \quad (A_{end} - f_{phen\_4\_FD}) < yd \le A_{end} \quad \text{(Eq. 6)}$$

where *yd* is the year day,
A_{start} and A_{end} are the year days for the start and end of the O_3 accumulation period respectively; parameters A_{start} and A_{end} and f_{phen_xx} are defined in the parametrization table (see Annex 1); the subscripts FD (e.g. A_{start_FD}) refer to the fixed day,
f_{phen_a}, f_{phen_e} is the phenology function, which consists of terms describing rate changes of g_{max} expressed as fractions (see Annex 1),
$f_{phen\_1\_FD}$, $f_{phen\_4\_FD}$ are °C days (see Annex 1; $f_{phen\_1\_FD}$ and $f_{phen\_4\_FD}$ define periods when trees are sensitive to O_3 exposure).

For beech in all modelled regions and for Norway spruce in the Boreal region, the start of the growing season is estimated using a simple latitude model and occurs at year day 105 at latitude 50°N, and alters by 1.5 days per degree latitude, starting earlier moving south and later moving north. The end of the growing season is estimated as occurring at year day 297 at latitude 50°N, and the end of the growing season will alter by 2 days per degree latitude, ending earlier moving north and later moving south. The effect of altitude on phenology is incorporated by assuming a later start of the growing season and earlier end of the growing season by 10 days for every 1 000 m.

$$A_{start\_FD} = 105 - 1.5 * (50 - latitude) + 10 * altitude/1000 \quad \text{(Eq. 7)}$$
$$A_{end\_FD} = 297 - 2 * (latitude - 50) - 10 * altitude/1000 \quad \text{(Eq. 8)}$$

It should be noted that there are currently discussions about the validity of this latitude model in some regions, although there is currently no immediate alternative approach available (CLRTAP, 2020).

For Norway spruce in the Continental region, the growth period is determined by air temperature defined according to the f_{temp} function. The growing season is assumed to occur when air temperatures are between the T_{min} and T_{max} thresholds of the f_{temp} relationships. During such periods there is no limitation on conductance associated with the leaf development stage (i.e. $f_{phen} = 1$).

The parameter f_{light} is calculated according to

$$f_{light} = 1 - EXP[(-light\_a)*PPFD] \quad \text{(Eq. 9)}$$

while
$$PPFD = SSRD * 0.5 * 4.5 \quad \text{(Eq. 10)}$$

where *light_a* depends on the species and biogeographical region (see Annex 1),
PPFD represents the photosynthetic photon flux density (µmol/m^2 per second),
SSRD represents the surface net solar radiation (W/m^2).

The parameter f_{temp} is calculated according to:

$$f_{temp} = \max\{f_{min}, [(T - T_{min}) / (T_{opt} - T_{min})] * [(T_{max} - T) / (T_{max} - T_{opt})]^{bt}\} \quad \text{for } T_{min} < T < T_{max} \quad \text{(Eq. 11)}$$

$$f_{temp} = f_{min} \quad \text{for } T < T_{min} \text{ or } T > T_{max} \quad \text{(Eq. 12)}$$

while
$$bt = (T_{max} - T_{opt}) / (T_{opt} - T_{min}) \quad \text{(Eq. 13)}$$

where T_{min}, T_{max} and T_{opt} are minimum, maximum and optimum temperatures determining leaf stomata opening (see Annex I).

The parameter f_{VPD} is calculated according to:

$$f_{VPD} = \min\{1,\max\{f_{min}, [(1-f_{min})*(VPD_{min} - VPD) / (VPD_{min} - VPD_{max})] + f_{min}\}\} \quad \text{(Eq. 14)}$$

while $VPD = e_s(Ta) * (1-hr)$ (Eq. 15)

$e_s(Ta) = a \exp [bT_a/(T_a+c)]$ (Eq. 16)

where VPD_{min} is the minimum vapour pressure deficit determining leaf stomata opening (kPa),
VPD_{max} is the maximum vapour pressure deficit determining leaf stomata opening (kPa),
T_a is the air temperature (°C),
h_r is the relative humidity (%)/100,
$e_s(Ta)$ is the potential (saturation) water vapour pressure,
a, b, c are the empirical constants (a = 0.611 kPa, b = 17.502, c = 240.97°C).

The parameter f_{SW} is replaced by f_{SMI}, (where *SMI* represents Soil Moisture Index with maximum at field capacity), taking values between 0 and 1 as a proportion of g_{max} (with 0 for soil moisture at and below wilting point). The basic equation used for f_{SW} resp. f_{SMI} is:

$$f_{SMI} = 0 \quad \text{for SMI} \leq 0 \quad \text{(Eq. 17)}$$

$$f_{SMI} = \frac{SMI}{SMI_t} \quad \text{for } 0 < \text{SMI} \leq SMI_t \quad \text{(Eq. 18)}$$

$$f_{SMI} = 1 \quad \text{for SMI} > SMI_t \quad \text{(Eq. 19)}$$

when $SMI = (SWLL - PWP) / (FC - PWP)$ (Eq. 20)

where SMI_t is the threshold SMI, set to 0.5, above which stomatal conductance is at a maximum,
SWLL is the soil moisture in (m^3/m^3),
PWP is the permanent wilting point in (cm^3/cm^3),
FC is the field capacity in (cm^3/cm^3).

The Soil Moisture Index using the EMEP methodology as described in Simpson et al. (2012) and CLRTAP (2020) is used. The index SMI has the advantage over volumetric methods that it is less sensitive to local soil characteristics, and hence is easier to interpolate across different vegetation types and grids (Simpson et al., 2012). It is computed using the soil moisture variable available from a meteorological model, which represents the water content in m^3 of water per m^3 of ground (m^3/m^3) at a specific ground level, in dependence on the available dataset. For soil moisture, the ECWMF's ERA5-Land variable Volume of water in soil layer 3 (i.e. 28-100 cm) has been used for beech and in soil layer 2 (i.e. 7-28 cm) for Norway spruce, see Section 3.3. The level of soil layer was chosen based on recommendations of Forestry and Game Management Research Institute (Novotný, personal communication, February 2, 2022) and also based on the results of Schmid (2002), Kodrík and Kodrík (2002), and Oravcová and Vido (2022).

The soil moisture is quite a sensitive parameter in the calculation of the POD. Next to the soil moisture, the soil moisture index also takes into account the permanent wilting point and the field capacity; they are taken from the JRC soil database (JRC, 2016), see Section 3.5.

The f_{SW} resp. f_{SMI} values used in EMEP-DO3SE are a very simple function of SMI, which itself is a simple scaling between the field capacity (FC) and permanent wilting point (PWP) of the vegetation. The ECMWF values of SMI, PWP and FC are per grid square, and thus not specific to any particular vegetation or soil.

2.1.4 Modelling the hourly stomatal flux of O_3 (F_{sto})

Once all variables of Section 2.1.3 are computed, the stomatal flux of O_3 (F_{sto}) can be calculated, based on the assumption that the concentration of O_3 at the top of the canopy represents a reasonable estimate of the concentration at the upper surface of the laminar layer for a sunlit upper canopy leaf. F_{sto} is calculated according to the ICP Vegetation methodology, thus the fraction of the O_3 taken up by the stomata is given using a combination of the stomatal conductance, the external leaf, or cuticular, resistance, the leaf

surface resistance, and the quasi-laminar resistance. The hourly stomatal flux at a given hour H is calculated according to

$$F_{sto} = c(z_{tgt}) * g_{sto} * \frac{r_c}{r_b + r_c} \quad \text{(Eq. 21)}$$

where
- F_{sto} is the hourly stomatal flux of O_3 in (nmol/m^2 PLA per second),
- $c(z_{tgt})$ is the concentration of O_3 at canopy top (nmol/m^3),
- r_b is the quasi-laminar resistance in (s/m),
- r_c is the leaf surface resistance in (s/m),
- g_{sto} is the actual stomatal conductance in (m/s),

while

$$r_c = 1/(g_{sto} + g_{ext}) \quad \text{(Eq. 22)}$$

$$g_{ext} = 1/2500 \text{ (m s}^{-1}\text{)} \quad \text{(Eq. 23)}$$

$$r_b = 1.3 * 150 * \sqrt{\frac{L}{\frac{u*}{k} \cdot \ln\left(\frac{z_{tgt}}{z_{0,tgt}}\right)}} \quad \text{(Eq. 24)}$$

where
- L is the cross-wind leaf dimension (cm, see Annex 1),
- $u*$ is the friction velocity (m/s),
- k is the von Kármán constant (equal to 0.41),
- z_{tgt} is the top of the canopy (m),
- $z_{0, tgt}$ is the roughness length, usually assumed as 1/10 of the canopy height (m).

2.1.5 Conversion of stomatal conductance (g_{sto}) and O_3 concentration to units required for PODy calculation

According to CLRTAP (2017a), stomatal conductance g_{sto} has to be converted from mmol/m^2 per second to m/s (since all the resistances are expressed in s/m). At standard temperature (20 °C) and air pressure (1.013 x 10^5 Pa), the conversion is made by dividing the conductance value expressed in mmol/m^2 per second by 41 000 to give conductance in m/s. To convert the O_3 concentration ($c(z_{tgt})$) at canopy height from µg/m^3 resp. ppb to nmol/m^3, the following equation should be used:

$$c(z_{tgt}) \text{ [nmol/m}^3\text{]} = c(z_1) \text{ [ppb]} * P/(R \cdot T) = c(z_{tgt}) \text{ [µg/m}^3\text{]} / 2 * P/(R \cdot T) \quad \text{(Eq. 25)}$$

where
- P is the atmospheric pressure in Pa,
- R is the universal gas constant of 8.31447 J mol/K
- T is the air temperature in Kelvin.

At standard temperature (20 °C) and air pressure (1.013 x 10^5 Pa), the concentration in ppb should be multiplied by 41.56 to calculate the concentration in nmol/m^3.

In the routine used in this paper (Section 2.3), an alternative conversion of the O_3 concentrations from µg/m^3 or ppb to nmol/m^3 is done, using the air density instead of the atmospheric pressure, according to

$$C \text{ [nmol/m}^3\text{]} = C \text{ [ppb]} * \rho / N_a * 10^6 = C \text{ [µg/m}^3\text{]} / 2 * \rho / N_a * 10^6 \quad \text{(Eq. 26)}$$

where
- ρ is the air density showing the number of the molecules per cm^3
- N_a is the Avogadro constant, which is equal to 6.022×10^{23} per mol

2.1.6 Calculation of POD_Y (POD_YSPEC or POD_YIAM) from F_{sto}

Hourly averaged stomatal O_3 fluxes (F_{sto}) in excess of a Y threshold are accumulated over a species or vegetation-specific accumulation period using the following equation:

$$\mathrm{POD_Y} = \sum_n (F_{sto}(n) - Y) \cdot \frac{3600}{10^6} (\mathrm{mmol/m^2\ PLA}) \qquad \text{(Eq. 27)}$$

while Y (for trees) = 1 nmol/m^2 PLA per second

where POD_Y is the phytotoxic O_3 dose related to the threshold *Y*, in mmol/m^2 PLA,
$F_{sto}(n)$ is the hourly O_3 flux in the hour *n*.

The value Y (nmol/m^2 PLA per second) is subtracted from each hourly averaged F_{sto} (nmol/m^2 PLA per second) value only when F_{sto} > Y, during daylight hours assessed as being when global radiation is more than 50 W/m^2. The value is then converted to hourly fluxes by multiplying by 3 600 and to mmol by dividing by 10^6 to get the stomatal O_3 flux in mmol/m^2 PLA.

2.1.7 Calculation of exceedance of flux-based critical levels

If the calculated POD_Y value is larger than the flux-based critical level for O_3, then there is exceedance of the critical level ($CL_{exceedance}$). Exceedance of the critical level is calculated at follows:

$$CL_{exceedance} = POD_Y - \text{critical level} \qquad \text{(Eq. 28)}$$

The species-group or species-specific flux models, associated response functions and critical levels for forest trees were derived from experiments with young trees and can be used to quantify the potential negative impacts of O_3 on the annual growth of the living biomass of trees at the local and regional scale.

The critical levels for forest trees were set to values for an acceptable biomass loss.

The critical level (CL) for beech is set to be 5.2 mmol/m^2 PLA (potential effect at this CL is a 4 % annual reduction of the whole tree biomass). The critical level for Norway spruce is set be to 9.2 mmol/m^2 PLA (potential effect at this CL is a 2 % annual reduction of the whole tree biomass).

2.2 Ozone gridded data estimation

The hourly O_3 gridded data (used in the POD mapping) are calculated by combining the monitoring, chemical transport modelling and other supplementary data. The methodology for this combination is a linear regression model followed by kriging of the residuals produced from that model (residual kriging), as routinely used in the hourly O_3 mapping applied in the regular POD for crops map creation (Horálek et al., 2022). Interpolation is therefore carried out according to the relation:

$$\hat{Z}(s_0) = c + a_1 X_1(s_0) + a_2 X_2(s_0) + \cdots + a_n X_n(s_0) + \eta(s_0) \qquad \text{(Eq. 29)}$$

where $\hat{Z}(s_0)$ is the estimated value of the air pollution indicator at the point s_o,
$X_1(s_0), X_2(s_0),\ldots, X_n(s_0)$ are *n* number of individual supplementary variables at the point s_o
$c, a_1, a_2,\ldots, a_n$ are *n+1* parameters of the linear regression model calculated based on the data at the points of measurement,
$\eta(s_0)$ is the spatial interpolation of the residuals of the linear regression model at the point s_o calculated based on the residuals at the points of measurement.

The gridded data are calculated for hourly values at 2×2 km^2 resolution, based on rural background measurements (see Section 3.1). The supplementary variables used are chemical transport model (CTM) output, surface solar radiation and altitude (see Sections 3.2-3.4).

2.3 Routines used

A module using R Software (R Core Team 2020) to estimate phytotoxic O_3 doses from a given atmospheric O_3 exposure as developed for the Continental biogeographical region by the INERIS (Colette et al., 2018) has been used. This script has been consolidated and finalized by the CHMI for use in the POD spatial calculation for selected trees, i.e. it has been modified also for use in the Boreal biogeographical region in the case of spruce and for the Mediterranean biogeographical region in the case of beech. It follows precisely the methodology and parametrisation described in the Manual for modelling and mapping critical loads & levels of the Air Convention (CLRTAP) in its most recent available revision dated 2017 (CLRTAP, 2017a).

The POD annual maps are calculated based on hourly O_3 gridded data (see Section 2.2), hourly meteorological data (Section 3.3) and the soil hydraulic properties data (Section 3.4).

3 The Input data

The input data for the POD calculation are the same as used for the regular mapping of POD for crops for 2020 (Horálek et al., 2022).

3.1 Air quality monitoring data

Air quality monitoring station data have been extracted from the official EEA Air Quality e-Reporting database (EEA, 2022). The data come from the E1a data flow, i.e. these are the official data as reported by the EEA's member and cooperating states. This data set has been supplemented with several EMEP rural stations from the EBAS database (NILU, 2022) which are not reported to the Air Quality e-Reporting database. Only data from stations classified as rural background have been considered. Ozone hourly data for 2020 have been used. In total, data from 549 monitoring stations have been applied, including 18 British stations from the EBAS database that are not included in the AQ e-reporting database. These ozone monitoring data have been used for the O_3 hourly gridded data estimation (see Section 2.2), together with the O_3 hourly modelling data and other supplementary data.

3.2 Chemical transport model output

The chemical dispersion modelling data used for the O_3 hourly gridded data estimation (see Section 2.2) are the CAMS Ensemble Forecast modelling O_3 hourly data. The output data of the CAMS modelling are provided by the Copernicus Atmosphere Monitoring Service (CAMS) at a regional scale over Europe. The European regional production consists of an ensemble of nine air quality models run operationally. The model forecasts of the individual models are combined into the Ensemble Forecast by taking the median of all nine models. For details of the individual models, see Marécal et al. (2015). All the models used in the CAMS ensemble products were run using the TNO-MACC emissions representative of 2011 (Kuenen et al., 2014) and the meteorology (i.e., the weather forecast) provided by the European Centre for Medium Range Weather Forecasts (ECMWF) operationally. The resolution of the modelling data is 0.1°×0.1° which is around 10×10 km.

3.3 Meteorological data

The meteorological data used are the ECWMF data extracted from the CDS (Climate Data Store, https://cds.climate.copernicus.eu/cdsapp#!/home). Hourly data for 2020 are used. Most of the data come from the reanalysed data set ERA5-Land at 0.1°x0.1° resolution, namely the indicators:

Surface solar radiation – variable "Surface solar radiation downwards"

Temperature – variable "2m temperature"

Soil water – variable "Volumetric soil water layer 3", i.e. layer of 28-100 cm for beech and "Volumetric soil water layer 2", i.e. layer of 7-28-100 cm for Norway spruce

Wind speed (WV) is derived from "10m u-component of wind" (10U) and "10m v-component of wind" (10V) according to relation

$$WV = \sqrt{(10U)^2 + (10V)^2} \quad \text{(Eq. 30)}$$

Relative humidity (RH) is derived by means of the saturated water vapour pressure (e_t) as a function of "2m temperature" (2T) and "2m dew point temperature" (2D) according to relation

$$RH = \frac{e_{2D}}{e_{2T}} \cdot 100, \text{ with } e_t = 6.1365^{\frac{17.502 \cdot t}{24097+t}} \quad \text{(Eq. 31)}$$

where *t* is 2T and 2D, respectively.

In the coastal areas (where the data from ERA5-Land are not available), the same parameters from the reanalysed data set ERA5 at 0.25°x0.25° resolution are applied. Additionally to this, the following data (not available in the ERA5-Land data set) from the ERA5 data set are also used:

Friction velocity [m/s] – variable "Friction velocity". The friction velocity (also known as the *shear-stress velocity*) has the dimensions of velocity, i.e. m/s.

Besides the ERA5-Land and ERA5 meteorological data, the following indicator, an output of the CHIMERE (Menut et al., 2021) pre-processing which uses ECWMF's IFS (Integrated Forecasting System) meteorological data as input, is used as hourly data for 2020 at 0.1×0.1° resolution:

Air density (molec/cm^3) – expressed the number of the molecules in cm^3.

All meteorological data were re-gridded and converted into the reference EEA 1×1 km^2 grid, 10×10 km^2 grid and 2×2 km^2 grid, in the ETRS89-LAEA5210 projection.

3.4 Altitude

We use the altitude data field (in m) of Global Multi-resolution Terrain Elevation Data 2010 (GMTED2010), with an original grid resolution of 15×15 arcseconds from U.S. Geological Survey Earth Resources Observation and Science, see Danielson et al. (2011). The original data were converted into the 2×2 km^2 grid resolution of the ETRS 1989 LAEA projection.

3.5 Soil hydraulic properties

JRC data labelled as "Maps of indicators of soil hydraulic properties for Europe" at 1×1 km^2 resolution are used; the dataset and maps have been downloaded from the European Soil Data CentreJRC (2016). The following indicators are used:

Wilting Point – water content at wilting point (cm^3/cm^3)
Field Capacity – water content at field capacity (cm^3/cm^3)

4 Results – maps of POD for beech and spruce

Maps 4.1 and 4.2 present the final maps of Phytotoxic Ozone Dose (POD_1) for beech and spruce respectively, in 2020. High values of POD_1 can be found across various areas of Europe, since POD_1 is dependent not only on O_3 levels but also on the environmental conditions and plant phenology. For example higher POD_1 values can occur in areas with lower O_3 concentrations but favourable conditions for the stomatal conductance. On the other hand, the lowest levels of POD_1 usually occur in areas with lower O_3 concentrations, such as northern European regions, and/or in areas where environmental conditions limit the O_3 stomatal conductance such as dry and warm areas, including parts of the southern and south-eastern Europe.

As with the maps of other vegetation-related indicators (Horálek et al., 2022), only monitoring data from the rural background stations are used in the mapping. Thus, the maps are representative for rural areas only, and the estimated POD values in the urban areas are based on the O_3 modelling data without adjustment by the monitoring data from the urban and suburban stations.

Map 4.1: Phytotoxic Ozone Dose (POD_1) for beech, rural map, 2020

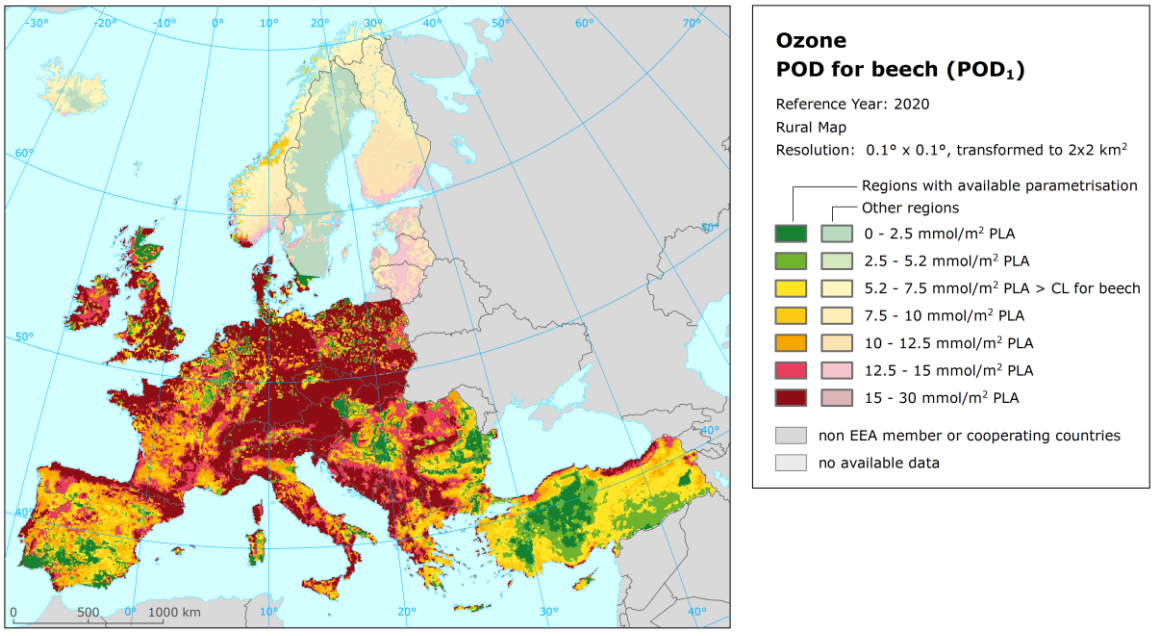

The areas in Map 4.1 with POD_1 values below the Critical Level (CL) for beech (i.e. 5.2 mmol/m^2 PLA) are marked in dark green and green. The areas with POD_1 values above the CL for beech are marked in yellow, dark yellow, orange, red and dark red. Since no parametrization for beech in the Boreal, Arctic and Alpine > 50° biogeographical regions is available, these areas are marked in lighter colours (see Section 2.1.1).

The CL for beech has been exceeded almost throughout the whole European area mapped, while some areas with POD_1 values below CL are found mainly in the Iberian Peninsula, Belgium, the United Kingdom, Austria, Serbia, Romania and Turkey.

The highest levels of POD_1 for beech in 2020 are found in western Europe (the United Kingdom and the Brittany region of France), in northern Europe (Denmark), in central Europe (parts of Germany, Czechia, Slovakia, Austria and Switzerland), parts of southern and south-eastern Europe (the north of Spain, parts of Italy, areas of the Balkan countries and the north of Turkey).

Map 4.2: Phytotoxic Ozone Dose (POD_1) for spruce, rural map, 2020

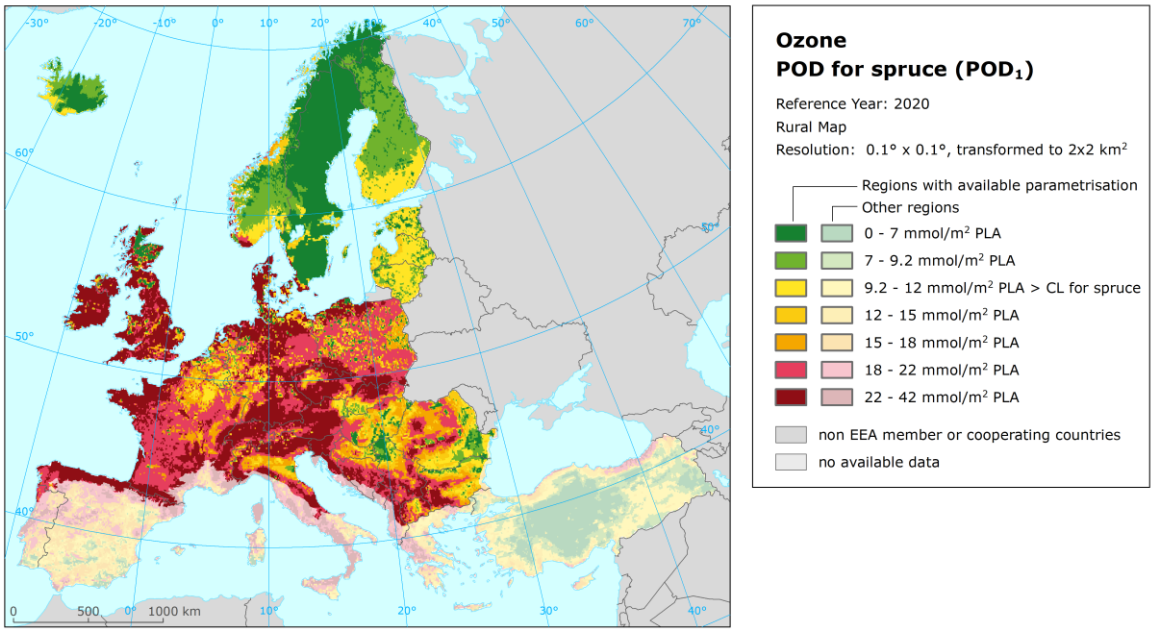

The areas in Map 4.2 with POD_1 values below the Critical Level (CL) for spruce (i.e. 9.2 mmol/m^2 PLA) are marked in dark green and green. The areas with POD_1 values above the CL for spruce are marked in yellow, dark yellow, orange, red and dark red. Since no parametrization for spruce in the Mediterranean, Anatolian and Black Sea biogeographical regions is available, this area is marked in lighter colours (see Section 2.1.1).

The CL for spruce has been exceeded almost throughout the whole European area mapped, with the exception of large areas in northern Europe, and some areas in the north of the United Kingdom and the Balkan countries. Nevertheless, according to CLRTAP (2020), the start of the growing season in northern Europe is earlier than the start of the growing season calculated by the current recommended latitude model. As a result of this earlier start of the growing season, POD_1 values in northern Europe could be higher than those presented. Unfortunately, a better approach for the start of the growing season for spruce is not currently available. Other small areas with values below the CL POD_1 are also found in the Benelux, France, Germany, Poland, Hungary, Slovakia and Italy.

The highest levels of POD_1 for spruce in 2020 are found in western Europe (the United Kingdom and France), in southern Europe (the north of Spain and parts of Italy), in south-eastern Europe (parts of different Balkan countries), in central Europe (parts of Switzerland, Germany, Czechia, Slovakia, Hungary, and Austria). High POD_1 is also seen in Denmark.

Conclusion

This paper examines the potential inclusion of the Phytotoxic Ozone Dose (POD) for selected trees in regular mapping under the ETC HE, following the earlier inclusion of the POD for crops (POD_6 for wheat, potato and tomato, see Horálek et al., 2021). Such an inclusion would be beneficial, as the flux-based POD_Y metrics (i.e. POD above a threshold flux Y) are generally preferred in risk assessment over the concentration-based exposure metrics like AOT40 indexes (Mills et al., 2011).

Maps of POD_1 for tree species of beech and spruce have been prepared, for a uniform species-independent O_3 flux threshold of Y = 1 nmol/m^2 PLA per second. The methodology applied is documented in detail and the input data used are fully detailed. POD calculation has been performed using routines developed earlier by INERIS (POD parametrisation for the Continental biogeographical region) and slightly modified by CHMI with the addition of POD parametrisation for the Boreal and Mediterranean biogeographical regions. This tool follows the methodology described in the Manual for modelling and mapping critical loads and levels of the Air Convention (CLRTAP) in its most recent available revision dated 2017 (CLRTAP, 2017a).

The POD maps have been constructed at 0.1° x 0.1° resolution, the final outputs were transferred to the 2x2 km^2 resolution of the EEA layout as routinely used in other regular maps of vegetation-related indicators. It can be concluded that the inclusion of POD for selected trees in routine mapping along with the other maps already produced is feasible. Thus, it is recommended to include POD_1 for beech and spruce in the routinely mapped air quality indicators. In future, addition of POD_1 for another tree species might be considered, preferably POD_1 for oak.

List of abbreviations

Abbreviation	Name	Reference
AOT40	Accumulated Ozone exposure over a Threshold of 40 ppb (i.e. 80 µg/m³) in a specific period	http://eur-lex.europa.eu/LexUriServ/LexUriServ.do?uri=OJ:L:2008:152:0001:0044:EN:PDF
CDS	Climate Data Store	https://cds.climate.copernicus.eu/cdsapp#!/home
CL	Critical Level	https://icpvegetation.ceh.ac.uk/chapter-3-mapping-critical-levels-vegetation
CLRTAP	Convention on Long-range Transboundary Air Pollution (Air Convention)	https://unece.org/environment-policy/air
ECMWF	European Centre for Medium-Range Weather Forecasts	https://www.ecmwf.int/
EEA	European Environment Agency	www.eea.europa.eu
EIONET	The European Environment Information and Observation Network	https://www.eionet.europa.eu/
EMEP	European Monitoring and Evaluation Programme	https://www.emep.int/
ETC HE	European Topic Centre on Human health and the environment	https://www.eionet.europa.eu/etcs/etc-he
EU	European Union	https://european-union.europa.eu
FC	Field capacity	https://icpvegetation.ceh.ac.uk/sites/default/files/Scientific%20Background%20document%20B%20June%202020.pdf
GIZ	Deutsche Gesellschaft für Internationale Zusammenarbeit (GIZ) GmbH	https://www.giz.de/
CHMI	Czech Hydrometeorological Institute	https://www.chmi.cz/
ICP	International scientific Cooperative Programme	https://icpvegetation.ceh.ac.uk/
INERIS	Institut national de l'environnement industriel et des risques (The French National Institute for Industrial Environment and Risks)	https://www.ineris.fr/fr
JRC	Joint Research Centre	https://ec.europa.eu/info/departments/joint-research-centre_en
NILU	Norwegian Institute for Air Research	https://www.nilu.no/
PLA	Projected Leaf Area	https://icpvegetation.ceh.ac.uk/chapter-3-mapping-critical-levels-vegetation
POD	Phytotoxic Ozone Doze	https://icpvegetation.ceh.ac.uk/chapter-3-mapping-critical-levels-vegetation
PWP	Permanent wilting point	https://icpvegetation.ceh.ac.uk/sites/default/files/Scientific%20Background%20document%20B%20June%202020.pdf

References

Agyei, T., et al., 2020, 'The impact of drought on total ozone flux in a mountain Norway spruce forest', *Journal of Forest Science* 66, pp. 280-278 (https://doi.org/10.17221/129/2019-JFS) accessed 28 March 2022.

Anav, A., et al., 2016, 'Comparing concentration-based (AOT40) and stomatal uptake (PODY) metrics for ozone risk assessment to European forests', *Global Change Biology* 22, pp. 1608–1627 (https://doi.org/10.1111/gcb.13138) accessed 27 April 2022.

Anav, A., et al., 2017, 'The role of plant phenology in stomatal ozone flux modeling' *Global Change Biology* 24, pp. 235–248 (https://doi: 10.1111/gcb.13823) accessed 13 February 2023.

Anav, A., et al., 2019, 'Growing season extension affects ozone uptake by European forests', *Science of The Total Environment* 669, pp. 1043-1052 (https://doi.org/10.1016/j.scitotenv.2019.03.020) accessed 11 July 2022.

Anav, A., et al., 2022, 'Legislative and functional aspects of different metrics used for ozone risk assessment to forests', *Environmental Pollution* 295(118690) (https://doi.org/10.1016/j.envpol.2021.118690) accessed 11 July 2022.

Ashmore, M. R., 2003, 'Surface Ozone Effects on Vegetation', in: Holton J.R., Curry J.A. and Pyle J.A. (eds), *Encyclopedia of Atmospheric Sciences*. Academic Press, Elsevier Science, Ltd., London. 1663–1671 p.

Ashmore, M.R., et al., 2005, 'Assessing the future global impacts of ozone on vegetation', *Plant, Cell and Environment* 28, pp. 949-964 (https://onlinelibrary.wiley.com/doi/epdf/10.1111/j.1365-3040.2005.01341.x) accessed 27 April 2022.

Büker, P., et al., 2012, 'DO3SE modelling of soil moisture to determine ozone flux to forest trees', *Atmospheric Chemistry and Physics* 12, pp. 5537-5562 (http://dx.doi.org/10.5194/acp-12-5537-2012) accessed 20 January 2023.

Büker, P., et al. , 2015, 'New flux based dose-response relationships for ozone for European forest tree species', *Environmental Pollution* 206, pp. 163-174 (https://doi.org/10.1016/j.envpol.2015.06.033) accessed 27 April 2022.

Cape, J. N., 2008, 'Surface ozone concentrations and ecosystem health: Past trends and a guide to future projections', Science of The Total Environment 400, pp. 257-269 (https://doi.org/10.1016/j.scitotenv.2008.06.025) accessed 9 February 2023.

Cieslik, S., 2009, 'Ozone fluxes over various plant ecosystems in Italy: a review', *Environmental Pollution* 157, pp. 1487-1496 (https://doi.org/10.1016/j.envpol.2008.09.050) accessed 26 May 2022.

CLRTAP, 2017a, *Manual for modelling and mapping critical loads & levels. Chapter III: "Mapping critical levels for vegetation"*, UNECE Convention on Long Range Transboundary Air Pollution, (https://icpvegetation.ceh.ac.uk/sites/default/files/FinalnewChapter3v4Oct2017_000.pdf) accessed 13 July 2022.

CLRTAP, 2017b, *Scientific Background Document A, Supplement of Chapter III (Mapping critical levels for vegetation) of the modelling and mapping manual of the LRTAP Convention* (https://icpvegetation.ceh.ac.uk/sites/default/files/ScientificBackgroundDocumentAOct2018.pdf) accessed 13 July 2022.

CLRTAP, 2020, *Scientific Background Document B, Developing areas of research and relevance to Chapter III (Mapping critical levels for vegetation) of the modelling and mapping manual of the LRTAP Convention* (https://icpvegetation.ceh.ac.uk/sites/default/files/Scientific%20Background%20document%20B%20June%202020.pdf) accessed 13 July 2022.

Coates, J., et al., 2016, 'The influence of temperature on ozone production under varying NOx conditions – a modelling study', Atmospheric Chemistry and Physics 16, pp. 11601–11615 (https://doi:10.5194/acp-16-11601-2016) accessed 3 February 2023.

Colette, A., et al., 2018, *Long term evolution of the impacts of ozone air pollution on agricultural yields in Europe. A modelling analysis for the 1990-2010 period*. Eionet Report – ETC/ACM 2018/15 European Environment Agency (https://www.eionet.europa.eu/etcs/etc-atni/products/etc-atni-reports/eionet_rep_etcacm_2018_15_o3impacttrends) accessed 28 August 2019.

Dalstein, L., et al., 2019, 'Ozone foliar damage and defoliation monitoring of P.cembra between 2000 and 2016 in the southeast of France', *Environmental Pollution* 244, pp. 451-461 (https://doi.org/10.1016/j.envpol.2018.10.081) accessed 26 May 2022.

Danielson, J. J. and Gesch, D. B., 2011, *Global multi-resolution terrain elevation data 2010 (GMTED2010)*, U.S. Geological Survey Open-File Report, pp. 2011-1073 (https://pubs.er.usgs.gov/publication/ofr20111073) accessed 19 November 2020.

De Marco, A., et al., 2017, 'Ozone exposure affects tree defoliation in a continental climate', *Science of The Total Environment* 596-597, pp. 396-404 (https://doi.org/10.1016/j.scitotenv.2017.03.135) accessed 11 July 2022.

EEA, 2015, *Air pollution due to ozone: health impacts and effects of climate change* (https://www.eea.europa.eu/data-and-maps/indicators/air-pollution-by-ozone-2/assessment) accessed 9 February 2023.

EEA, 2016, *Biogeographical regions in Europe* (http://www.eea.europa.eu/data-and-maps/data/biogeographical-regions-europe-3) accessed 26 September 2022.

EEA, 2022, *Air Quality e-Reporting. Air quality database* (https://www.eea.europa.eu/data-and-maps/data/aqereporting-9). Data extracted in March 2022.

Emberson, L. D., et al., 2000, 'Modelling stomatal ozone flux across Europe', *Environmental Pollution* 109, pp. 403-413 (https://doi.org/10.1016/S0269-7491(00)00043-9) accessed 26 May 2022.

EU, 2016, Directive (EU) 2016/2284 of the European Parliament and of the Council of 14 December 2016 on the reduction of national emissions of certain atmospheric pollutants, amending Directive 2003/35/EC and repealing Directive 2001/81/EC (*OJ L 344, 17.12.2016, p. 1-31*).

EU, 2019, Communication from the Commission — Commission Notice on ecosystem monitoring under Article 9 and Annex V of Directive (EU) 2016/2284 of the European Parliament and of the Council on the reduction of national emissions of certain atmospheric pollutants (NEC-Directive) (*OJ C 92, 11.3.2019, p. 1-18*).

Fares, S., et al., 2010, 'Ozone fluxes in a Pinus ponderosa ecosystem are dominated by non-stomatal processes: Evidence from long-term continuous measurements', *Agricultural and Forest Meteorology* 150, pp. 420-431 (https://doi.org/10.1016/j.agrformet.2010.01.007) accessed 28 March 2022.

Fares, S., et al., 2013, 'Testing of models of stomatal ozone fluxes with field measurements in a mixed Mediterranean forest', *Atmospheric Environment* 67, pp. 242-251 (https://doi.org/10.1016/j.atmosenv.2012.11.007) accessed 26 May 2022.

Fares, S., et al., 2018, 'Ozone flux in plant ecosystems: new opportunities for long-term monitoring networks to deliver ozone-risk assessments', *Environmental Science and Pollution Research* 25, pp. 8240–8248 (https://doi.org/10.1007/s11356-017-0352-0) accessed 11 July 2022.

Feng, Z., et al., 2019, 'Economic losses due to ozone impacts on human health, forest productivity and crop yield across China', Environment International 131, pp. 104966 (https://doi.org/10.1016/j.envint.2019.104966) accessed 3 February 2023.

Fuhrer, J., et al., 1997, 'Critical levels for ozone effects on vegetation in Europe', *Environmental Pollution* 97, pp. 91-106 (https://doi.org/10.1016/S0269-7491(97)00067-5) accessed 26 May 2022.

Gerosa, G., et al., 2003, 'Micrometeorological determination of time-integrated stomatal ozone fluxes over wheat: a case study in Northern Italy', *Atmospheric Environment* 37, pp. 777-788 (https://doi.org/10.1016/S1352-2310(02)00927-5) accessed 28 March 2022.

Gill, S.S. and Tuteja, N., 2010, 'Reactive Oxygen Species and Antioxidant Machinery in Abiotic Stress Tolerance in Crop Plants', *Plant Physiology and Biochemistry* 48, pp. 909-930 (https://doi.org/10.1016/j.plaphy.2010.08.016) accessed 28 March 2022.

Hendriks, C., et al., 2016, 'Ozone concentrations and damage for realistic future European climate and air quality scenarios', Atmospheric Environment 144, pp. 208–219 (http://dx.doi.org/10.1016/j.atmosenv.2016.08.026) accessed 9 February 2023.

Horálek, J., et al., 2021, *European air quality maps for 2019*, Eionet Report ETC/ATNI 2021/1 (https://doi.org/10.5281/zenodo.6241308) accessed 31 October 2022.

Horálek, J., et al., 2022, *European air quality maps for 2020*, Eionet Report ETC HE 2022/12 (https://www.eionet.europa.eu/etcs/etc-he/products/etc-he-report-2022-12-european-air-quality-maps-for-2020-pm10-pm2-5-ozone-no2-nox-and-benzo-a-pyrene-spatial-estimates-and-their-uncertainties) accessed 9 February 2023.

Hoshika, Y., et al., 2013, 'Photosynthetic response of early and late leaves of white birch (Betula platyphylla var. japonica) grown under free-air ozone exposure', *Environmental Pollution* 182, pp. 242-247 (https://doi.org/10.1016/j.envpol.2013.07.033) accessed 26 May 2022.

Jakovljević, T., et al., 2021, 'Impact of ground-level ozone on Mediterranean forest ecosystems health', *Science of The Total Environment* 783(147063) (https://doi.org/10.1016/j.scitotenv.2021.147063) accessed 27 April 2022.

Jarvis, P. G., 1976, 'The interpretation of the variation in leaf water potential and stomatal conductance found in canopies in the field', *Philosophical Transactions of the Royal Society of London*, Series B: Biological Sciences 273, pp. 593-610 (https://doi.org/10.1098/rstb.1976.0035) accessed 26 May 2022.

Jones, M.E., et al., 2004, 'Influence of ozone and nitrogen deposition on bark beetle activity under drought conditions', *Forest Ecology and Management* 200, pp. 67–76 (https://doi.org/10.1016/j.foreco.2004.06.003) accessed 11 July 2022.

JRC, 2016, *Maps of indicators of soil hydraulic properties for Europe*, dataset/maps downloaded from the European Soil Data Centre (http://esdac.jrc.ec.europa.eu/content/maps-indicators-soil-hydraulic-properties-europe) accessed 8 December 2020.

Kärenlampi, L. and Skärby, L. (eds), 1996, *Critical Levels for Ozone in Europe: Testing and Finalizing the Concepts*. University of Kuopio, Kuopio. 363 p.

Karlsson, P. E., et al., 2005, 'Economic Assessment of the Negative Impacts´of Ozone on Crop Yields and Forest Production. A Case Study of the Estate Östads Säteri in Southwestern Sweden', Ambio 34, pp. 32–40 (https://doi.org/10.1579/0044-7447-34.1.32) accessed 3 February 2023.

Karlsson, P. E., et al., 2017, 'Past, present and future concentrations of ground-level ozone and potential impacts on ecosystems and human health in northern Europe', Science of The Total Environment 576, pp. 22-35 (https://doi.org/10.1016/j.scitotenv.2016.10.061) accessed 26 May 2022.

Kodrík, J. and Kodrík, M., 2002, 'Root biomass of beech as a factor influencing the wind tree stability', *Journal of Forest Science* 48, pp. 549–564 (https://www.agriculturejournals.cz/publicFiles/286472.pdf) accessed 11 July 2022.

Kuenen, J. J. P., et al., 2014, 'TNO-MACC_II emission inventory; a multi-year (2003--2009) consistent high-resolution European emission inventory for air quality modelling', *Atmospheric Chemistry and Physics*, 14, pp. 10963–10976 (https://doi.org/10.5194/acp-14-10963-2014) accesed 16 February 2021.

Long, S.P. and Naidu, S.L., 2002, 'Effects ox oxidants at the biochemical, cell and physiological levels, with particular reference to ozone', in: Bell, J.N.B., Treshow, M., (eds), Air Pollution and Plant Life. John Wiley & Sons, Chichester.

Marécal, V., et al., 2015, 'A regional air quality forecasting system over Europe: The MACC-II daily ensemble production', *Geoscientific Model Development*, 8, pp. 2777–2813 (https://doi.org/10.5194/gmd-8-2777-2015) accesed 16 February 2021.

Matyssek, R., et al., 2007, 'Promoting the O3 flux concept for European forest trees', *Environmental Pollution* 146, pp. 587-607 (https://doi.org/10.1016/j.envpol.2006.11.011) accessed 11 July 2022.

Menut, L., et al., 2021, 'The CHIMERE v2020r1 online chemistry - transport model', *Geoscientific Model Development* 14, pp. 678-6811 (https://doi.org/10.5194/gmd-14-6781-2021) accessed 31 October 2022.

Michel, A., et al., 2021, *Forest Condition in Europe: The 2021 Assessment. ICP Forests Technical Report under the UNECE Convention on Long-range Transboundary Air Pollution (Air Convention).* Eberswalde: Thünen Institute. (https://doi.org/10.3220/ICPTR1624952851000) accessed 3 February 2023.

Mills, G., et al., 2011, 'New stomatal flux-based critical levels for ozone effects on vegetation', *Atmospheric Environment* 45, pp. 5064-5068 (https://doi.org/10.1016/j.atmosenv.2011.06.009) accessed 19 November 2020.

Mittler, R., 2002, 'Oxidative stress, antioxidants and stress tolerance', *Trends in Plant Science* 7, pp. 405-410 (https://doi.org/10.1016/S1360-1385(02)02312-9) accessed 27 April 2022.

Monks, P.S., et al., 2009, 'Atmospheric composition change – global and regional air quality', *Atmospheric Environment* 43, pp. 5268-5350 (https://doi.org/10.1016/j.atmosenv.2009.08.021) accessed 28 March 2022.

Musselman, R.C., et al., 2006, 'A critical review and analysis of the use of exposure- and flux-based ozone indices for predicting vegetation effects', *Atmospheric Environment* 40, pp. 1869–1888 (https://doi.org/10.1016/j.atmosenv.2005.10.064) accessed 11 July 2022.

Musselman, R. C. and Massman, W. J., 1998, 'Ozone flux to vegetation and its relationship to plant response and ambient air quality standards', *Atmospheric Environment* 33, pp. 65-73 (https://doi.org/10.1016/S1352-2310(98)00127-7) accessed 26 May 2022.

NILU, 2022, *EBAS, database of atmospheric chemical composition and physical properties* (http://ebas.nilu.no) accessed 11 April 2022.

Nussbaum, S., et al., 2003, 'High-resolution spatial analysis of stomatal ozone uptake in arable crops and pastures', *Environmental International* 129, pp. 385-392 (https://www.ncbi.nlm.nih.gov/pubmed/12676231) accessed 26 May 2022.

Oliver, J.R., 2018, 'Large but decreasing effect of ozone on the European carbon sink', *Biogeosciences* 15, pp. 4245–4269 (https://doi.org/10.5194/bg-15-4245-2018) accessed 3 February 2023.

Oravcová, Z. and Vido, J., 2022, 'Understanding the Complexity of Drought within the Soil Profile in Beech Ecosystems on Their Lower Altitudinal Limit in Slovakia', *Water* 14(1338) (https://doi.org/10.3390/w14091338) accessed 26 May 2022.

Paoletti, E., 2006, 'Impact of ozone on Mediterranean forests: A review', *Environmental Pollution* 144, pp. 463-474 (https://doi.org/10.1016/j.envpol.2005.12.051) accessed 26 May 2022.

Paoletti, E., et al., 2019, 'Toward stomatal–flux based forest protection against ozone: The MOTTLES approach', *Science of The Total Environment* 691, pp. 516-527 (https://doi.org/10.1016/j.scitotenv.2019.06.525) accessed 26 May 2022.

Paoletti, E. and Manning, W., 2007, 'Toward a biologically significant and usable standard for ozone that will also protect plants', *Environmental Pollution* 150, pp. 85-95 (https://doi.org/10.1016/j.envpol.2007.06.037) accessed 28 March 2022.

Pell, E.J., et al., 1997, 'Ozone induced oxidative stress: Mechanism of action and reaction', *Physiologia Plantarum* 100, pp. 264–273 (https://onlinelibrary.wiley.com/doi/pdf/10.1111/j.1399-3054.1997.tb04782.x) accessed 27 April 2022.

Proietti, C., et al., 2021, 'Trends in tropospheric ozone concentrations and forest impact metrics in Europe over the time period 2000–2014', *Journal of Forestry Research* 32, pp. 543–551 (https://doi.org/10.1007/s11676-020-01226-3) accessed 11 July 2022.

R Core Team, 2020, R: A language and environment for statistical computing. R Foundation for Statistical Computing, Vienna, Austria (https://www.R-project.org/).

Ronan, A.C., et al., 2020, 'Have improvements in ozone air quality reduced ozone uptake into plants? ', *Elementa: Science of the Anthropocene* 8(2) (https://doi.org/10.1525/elementa.399) accessed 26 May 2022.

The Royal Society, 2008, *Ground-Level Ozone in the 21st Century: Future Trends, Impacts and Policy Implications,* RS Policy document 15/08, The Royal Society, London (https://royalsociety.org/-/media/Royal_Society_Content/policy/publications/2008/7925.pdf) accessed 26 May 2022.

Sacchelli, S., et al., 2021, 'Economic impacts of ambient ozone pollution on wood production in Italy', Scientific Reports 11, pp. 154 (https://doi.org/10.1038/s41598-020-80516-6) accessed 3 February 2023.

Schmid, I., 2002, 'The influence of soil type and interspecific competition on the fine root system of Norway spruce and European beech', *Basic and Applied Ecology* 3, pp. 339-346 (https://doi.org/10.1078/1439-1791-00116) accessed 26 May 2022.

Schraudner, M., et al., 1997, 'Changes in the biochemical status of plant cells induced by the environmental pollotant ozone', *Physiologia Plantarum* 100, pp. 274-280 (https://doi.org/10.1111/j.1399-3054.1997.tb04783.x) accessed 26 May 2022.

Seinfeld, J. H., Pandis, S. N., 2006. *Atmospheric chemistry and physics: from air pollution to climate change, 2 nd edition.* New York: John Wiley & Sons, Inc. ISBN 978-0-471-72017-1.

Sicard, P., et al., 2016, 'An epidemiological assessment of stomatal ozone flux-based critical levels for visible ozone injury in Southern European forests', *Science of the Total Environment* 541, pp. 729–741 (https://doi.org/10.1016/j.scitotenv.2015.09.113) accessed 27 April 2022.

Sicard, P., et al., 2017, 'Projected global ground-level ozone impacts on vegetation under different emission and climate scenarios', *Atmospheric Chemistry and Physics* 17, pp. 12177–12196 (https://doi.org/10.5194/acp-17-12177-2017) accessed 27 April 2022.

Sillman, S., et al., 1990, 'The sensitivity of ozone to nitrogen oxides and hydrocarbons in regional ozone episodes', Journal of Geophysical Research: Atmospheres 9, pp. 1837–1851 (https://doi.org/10.1029/JD095iD02p01837) accessed 3 February 2023.

Simpson, D., et al., 2012, 'The EMEP MSC-W chemical transport model – technical description', *Atmospheric Chemistry and Physics* 12, pp. 7825-7865 (https://doi.org/10.5194/acp-12-7825-2012) accessed 26 August 2020.

Stanners, D., Bourdeau, P. (eds), 1995, *Europe´s Environment: The Dobris Assessment,* EEA, Copenhagen.

Tuovinen, J.P., et al., 2009, 'Modelling ozone fluxes to forests for risk assessment: status and prospects', *Annals of Forest Science* 66, pp. 401 (https://doi.org/10.1051/forest/2009024) accessed 9 February 2023.

Varotsos, K.V, et al., 2013, 'Assessment of the impacts of climate change on European ozone levels', *Water, Air and Soil Pollution* 224, pp. 1596 (http://dx.doi.org/10.1007/s11270-013-1596-z) accessed 9 February 2023.

Vollenweider, P., et al., 2003, 'Validation of leaf ozone symptoms in natural vegetation using microscopical methods', *Environmental Pollution* 124, pp. 101-118 (https://doi.org/10.1016/s0269-7491(02)00412-8) accessed 11 July 2022.

Wittig, V.E., et al., 2009, 'Quantifying the impact of current and future tropospheric ozone on tree biomass, growth, physiology and biochemistry: a quantitative meta-analysis', *Global Change Biology* 15, pp. 396–424 (https://doi.org/10.1111/j.1365-2486.2008.01774.x) accessed 11 July 2022

Zhang, Y., et al., 2022, 'Plants and related carbon cycling under elevated ground-level ozone: A mini review', *Applied Geochemistry* 144, p. 105400 (https://doi.org/10.1016/j.apgeochem.2022.105400) accessed 9 February 2023.

Annex 1

Table A1.1: Summary of the parameterisation for POD_1SPEC calculations of sunlit leaves at the top of the canopy of common beech (*Fagus sylvatica*) and Norway spruce (*Picea abies*) for different biogeographical regions

Parameter	Units				
Tree species		**Norway spruce**	**Norway spruce**	**Beech**	**Beech**
Region		**Boreal**	**Continental, Atlantic, Steppic, Pannonian**		**Mediterranean**
g_{max}	mmol O_3/m^2 PLA/s	125	130	155	155
f_{min}	fraction	0.1	0.16	0.13	0.02
light_a	NA	0.006	0.01	0.006	0.006
T_{min}	°C	0	0	5	4
T_{opt}	°C	20	14	16	21
T_{max}	°C	200 ([a])	35	33	37
VPD_{max}	kPa	0.8	0.5	1	1
VPD_{min}	kPa	2.8	3	3.1	4
A_{start}	°C day	Latitude model	f_{temp} ([b])	Latitude model	Latitude model
A_{end}	°C day	Latitude model	f_{temp} ([b])	Latitude model	Latitude model
Leaf dimension	cm	0.8	0.8	7	7
Canopy height	m	20	20	20 ([c])	20
f_{phen_a}	fraction	0	0	0	0
f_{phen_e}	fraction	0	0	0.4	0
f_{phen_1}	no. of days	20	0	20	15
f_{phen_4}	no. of days	30	0	20	20

Notes:
([a]) The T_{max} value is set at 200 °C to simulate the weak response to high temperatures of Norway spruce growing under Northern European conditions. Hence, the T_{max} value should be viewed as a forcing rather than descriptive parameter.
([b]) For continental Norway spruce, the growing season is assumed to occur when air temperatures are between the T_{min} and T_{max} thresholds of the f_{temp} relationships. During such periods there is no limitation on conductance associated with leaf development stage (i.e. $f_{phen} = 1$).
([c]) Canopy height is fixed to 25 m for beech in these regions in last version of the Manual for modelling and mapping critical loads and levels. Nevertheless, for this paper, the O_3 concentration at the canopy height is calculated using tabulated gradient set to the maximum canopy height of 20 m.

Source: CLRTAP, 2017a; CLRTAP, 2020.

Annex 2

Table A2.2: Summary of the parameterisation for POD_1SPEC calculations used for different biogeographical regions

Biographic regions in Europe (EEA, 2016)	Parameterisation (CLRTAP, 2017a, 2020) for beech *(F. sylvatica)*	Parameterisation (CLRTAP, 2017) for spruce *(P. abies)*
Alpine > 50°	(Continental)	Boreal
Alpine < 50°	Continental	Continental
Anatolian	Continental	(Continental)
Arctic	(Continental)	Boreal
Atlantic	Continental	Continental
Black Sea	Mediterranean	(Continental)
Boreal	(Continental)	Boreal
Continental	Continental	Continental
Mediterranean	Mediterranean	(Continental)
Pannonian	Continental	Continental
Steppic	Continental	Continental

Note: Regions presented in lighter colours in the Maps 4.1 and 4.2 are in brackets.

Map A2.1: Biogeographical regions in Europe

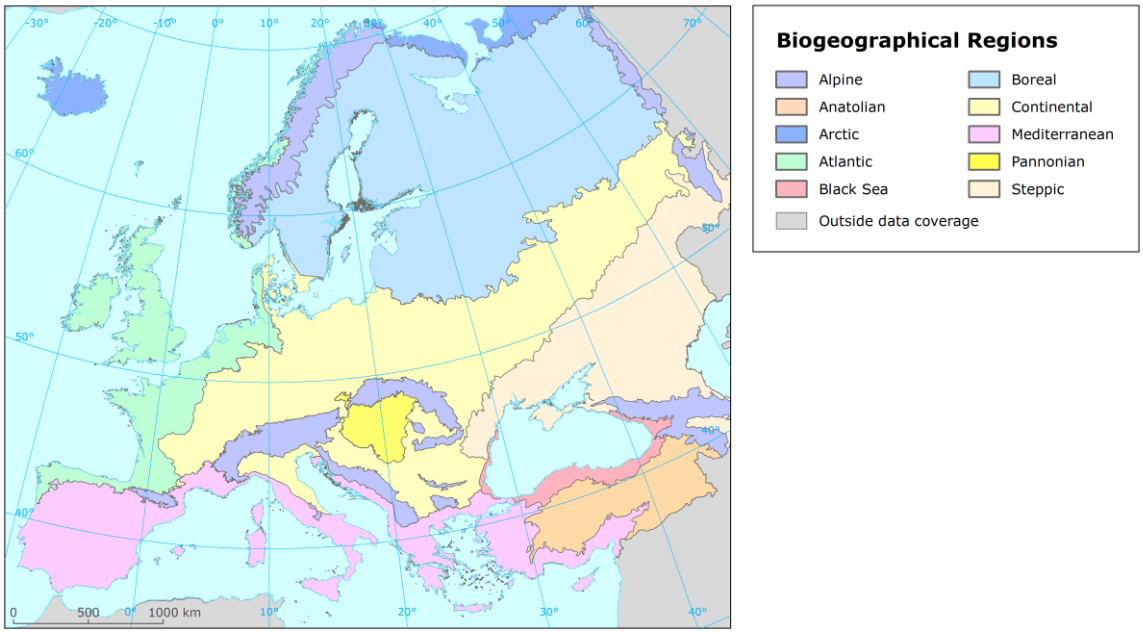

Source: EEA, 2016.

European Topic Centre on
Human health and the environment
https://www.eionet.europa.eu/etcs/etc-he

The European Topic Centre on Human health and the environment (ETC HE) is a consortium of European institutes under contract of the European Environment Agency.

European Environment Agency
European Topic Centre
Human health and the environment